#### Research Article

Hao Ming, Yinyan Guan, Cong Geng, Yingjun Gao, Jing Meng, and Jiyan Liang\*

# Rheological behavior of particle-filled polymer suspensions and its influence on surface structure of the coated electrodes

https://doi.org/10.1515/epoly-2023-0133 received August 23, 2023; accepted February 08, 2024

Abstract: Capacitive deionization electrode prepared by coating was commonly investigated, with polymer solution as binder and active particles as adsorbent. In the coating process, microstructure constituted by the two components was damaged by shear, then rebuilt when shear was removed. The microstructure strongly influenced the surface structure of the coated electrodes, further to performance and cycle life. The discussion of the interaction between the components in the coating process facilitates the identification of structural mechanisms. Rheology bridged the flow regimes in macroscale and interaction in microscale, through which the interaction between the polymer and particles can be investigated in a macroscopic phenomenon. In this study, hydrophilic polymer, poly(vinyl alcohol) (PVA), and poly(ethylene oxide) (PEO) were used as binders to prepare the suspension for coating. The influence of polymer molecular structure to interaction and microstructure was investigated by rheology. Results showed that the flexibility of polymer determined the adsorption morphology, leading to different flocculation structures. For rigid PVA, a 3d-crosslinked network was formed, giving a tough coating. While for flexible PEO, encapsulation structure was formed, leading to a brittle coating. A model based on bridging flocculation was evaluated to describe the formation and destruction of the flocculation structure. And a rheological method for binder selection and coating operation was proposed.

**Hao Ming:** School of Material Science and Engineering, Shenyang University of Technology, Shenyang 110870, China; Department of Environmental and Biological Engineering, Shenyang Institute of Science and Technology, Shenyang 110167, China

**Yinyan Guan, Cong Geng, Yingjun Gao, Jing Meng:** School of Material Science and Engineering, Shenyang University of Technology, Shenyang 110870, China

**Keywords:** capacitive deionization, coating method, rheology behavior, molecular flexibility, bridging flocculation

#### 1 Introduction

Capacitive deionization (CDI) is a promising desalting technique for medium and low concentration brine (1-4). The key part of the CDI system is the electrode (5), whose adsorption capacity depends on various factors, such as the specific capacitance, electrical resistance, pore structure, and surface functional groups (6-8). Moreover, the wettability and hydrophilicity of electrode also significantly influenced desalination performance (9). It confirmed that better wettability leads to sufficient contact between ions and electrode surface, and entire participating of pore due to the deep diffusion into the pore, contributing to the improvement of ion adsorption capacity (10). Various methods were used to improve the wettability, such as potassium hydroxide activation (11), metal oxide deposition (12), silica gel electrodes (13), and ionexchange resins (14).

Coated electrodes with polymeric binder were generally investigated (15,16). Since binder determined the mechanical strength, surface structures, and electrical conductivity, using hydrophilic polymers as binder is another effective way to improve the wettability (17,18). Among commercially available hydrophilic polymers, poly(vinyl alcohol) (PVA) (19–22) has been reported as a good candidate for improving the wettability of polymer-bonded electrodes. Due to the hydrophilic nature of the polymer, better performance was achieved.

The coating method using polymer as a binder has been widely used in the preparation of film electrode because of the simple process and suitability for large-scale industrial production. In the general preparation process, insoluble particles dispersed in polymer solution form a suspension as precursor (23). Polymer in the suspension adsorbed on the surface of particles leads to flocculent

<sup>\*</sup> Corresponding author: Jiyan Liang, School of Material Science and Engineering, Shenyang University of Technology, Shenyang 110870, China, e-mail: liangjiyan2017@126.com

structure, owing to entanglement, hydrogen bonding, and Van der Waals forces. During coating process, destruction and rebuilding of microstructure under shear gave suspension a particular rheological behavior. This behavior is associated with the film-forming and microstructure of electrode surface, which influence the performance. So far, materials, electrochemical properties, and desalination performance of CDI coated electrodes have been studied sufficiently (24), while research on the forming technology, structural transformation during molding process, and interaction between constituents in suspensions are still relatively far away from enough.

Rheological analysis was commonly used to investigate interaction and microstructure transformation in polymer melt, solution, and suspension, which bridged the flow regimes in macroscale and interaction in microscale (25,26). In this study, the influence of polymer on microstructure of coating was investigated utilizing this tool. Hydrophilic polymer, PVA, and poly(ethylene oxide) (PEO) were used as binders to prepare suspension for water-wettable films, in order to investigate the influence of molecular structure, which played an important role in microstructure change under shear. Combining with the surface structure of films, applicable rheological behavior of suspension for coating was achieved.

#### 2 Materials and methods

#### 2.1 Materials

PVA ( $M_{\rm w} \sim 7.56 \times 10^4~{\rm g\cdot mol}^{-1}$ , 98–99% alcoholysis degree) and PEO ( $M_{\rm w} \sim 1 \times 10^5~{\rm g\cdot mol}^{-1}$ ) were purchased from Aladdin Industrial Corporation in Shanghai, China. Ludox TM-50 colloidal silica (average diameter of 22 nm, 50 wt%) was obtained from Sigma-Aldrich in the USA. All reagents were used as received without further purification, and deionized water was used in all experiments.

#### 2.2 Suspensions preparation

To prepare the suspensions, PVA or PEO and silica nanoparticles were used following a specific preparation protocol. First, 6 g of PVA powder was added to 94 g deionized water and continuously mechanically stirred at 95°C for 48 h (≤100 rad·min<sup>-1</sup>) to prepare a homogeneous aqueous polymer solution with a mass concentration of 6%w/w.

A similar operation was performed for PEO blank solution, but at room temperature. Next, colloidal silica was added to the polymer solution in batches to achieve the desired concentrations; the amount of single addition was about 1 g with an interval of 1 h. The mixture was then continuously mixed for at least 24 h (≤100 rad·min⁻¹, room temperature) to break silica agglomerates and to ensure a homogeneous suspension. The concentration of polymer was 6%w/w, while the concentrations of silica nanoparticles were 20, 25, 30, and 35%w/w. The samples were left to rest for more than 1 day before use. All the sample codes used are shown in Table 1.

#### 2.3 Rheological measurements

Rheological measurements were performed using an Anton Paar MCR102 rheometer (Graz, Austria) with parallel plates (25 mm diameter, 316L stainless steel). The parallel plates are spaced 1.0 mm apart. Viscosity measurements were conducted within the range of 1–100 s<sup>-1</sup>, taking into account the possible coating velocity. Dynamic viscoelastic modulus measurements included frequency sweep (strain amplitude of 0.1%, frequencies ranging from 0.158 to 100 rad·s<sup>-1</sup>) and amplitude sweep (angular frequency of 6.28 s<sup>-1</sup>, strain amplitudes ranging from 0.01% to 100%). The three-interval Thixotropy Test (3ITT) consisted of pre-shear and three intervals. Pre-shear for 20 s (shear rate of 0.25 s<sup>-1</sup>) was performed to eliminate the timedependent changes of suspensions. The three intervals were in order of rest interval for 50 s (constant small shear rate of 0.5 s<sup>-1</sup>), load interval for 50 s (high shear rate of 100 s<sup>-1</sup>), and a recovery interval for 300 s (shear rate returned to 0.5 s<sup>-1</sup>). The hysteresis loop measurements were obtained by increasing the shear rate from 0 to 100 s<sup>-1</sup> for 300 s and decreasing it from 100 to 0 s<sup>-1</sup> for 300 s. The temperature was maintained at 25°C for all runs.

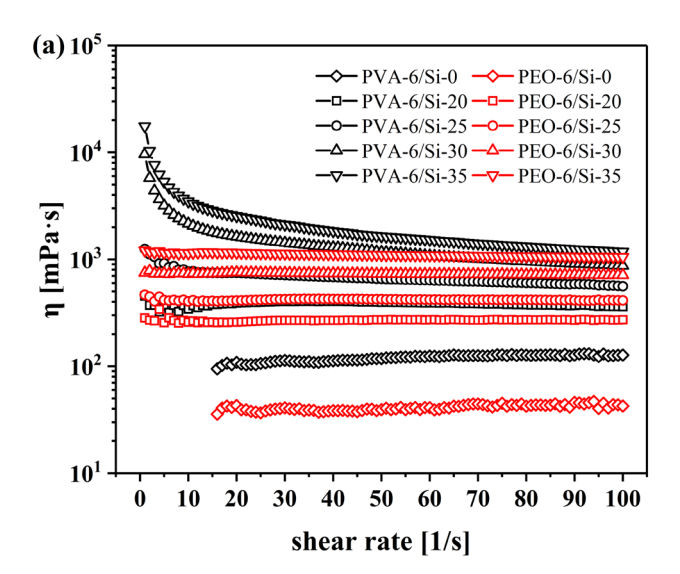
Table 1: Sample codes used in the experiment

Sample ID	Polymer	Silica concentration (%w/w)
PVA-6/Si-20	PVA	20
PVA-6/Si-25	PVA	25
PVA-6/Si-30	PVA	30
PVA-6/Si-35	PVA	35
PEO-6/Si-20	PEO	20
PEO-6/Si-25	PEO	25
PEO-6/Si-30	PEO	30
PEO-6/Si-35	PEO	35

#### 3 Results and discussions

#### 3.1 Steady shear of suspensions

Figure 1 displays the shear rate dependence of suspensions with varying particle concentrations. The PVA or PEO blank media without mixed particles are mostly Newtonian with a low viscosity. It was obvious that the addition of silica nanoparticles leads to an increase in viscosity across the whole range of shear rates regardless of the polymer used. As viscosity reflects the friction between adjacent layers in liquid, the addition of particles increased the friction between polymer molecules, due to the inhibiting role in motion of polymer chain segments (27). As a result, a thickening effect to polymer suspension was



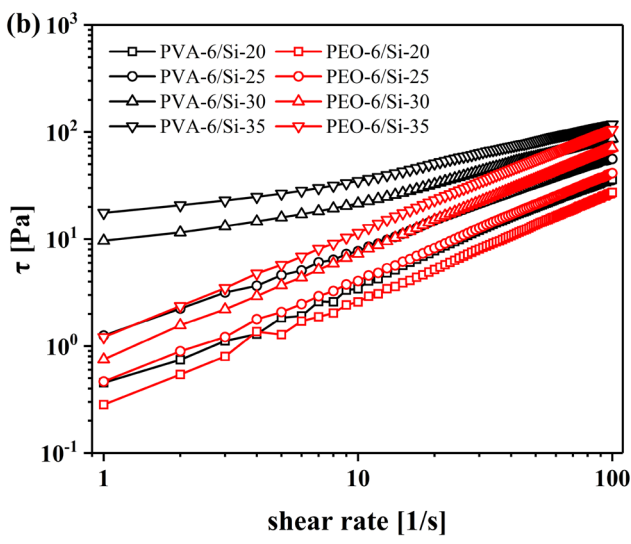


**Figure 1:** Flow curve of PVA/SiO $_2$  and PEO/SiO $_2$  suspensions: (a) viscosity vs shear rate and (b) shear stress vs shear rate.

observed. According to Eisenberg's model, the interaction of polymer segments with silica reduces the mobility of polymer and results in the formation of immobilized and restricted mobility regions around the filler particles (28).

There were differences between PVA and PEO. For PVA, as the silica increases, the suspension changes from Newtonian fluid to shear-thinning fluid. While for PEO, the suspension was still Newtonian fluid even though the silica increased as much as 35%w/w. Since the molecular weights of PVA and PEO used were similar, the different response of viscosity to particle concentration was attributed to function group and structure. Figure 2 shows the molecular structures of the two polymer binders.

Both PVA and PEO are linear polymers, whose conformation in solution can be described through the random walk concept to be a flexible coil. In suspensions, when the polymer coil approaches the surface of the particle, the polymer segment replaces the solvent on the particle surface and adsorbed with conformation transition (29). Relevant studies proposed that the adsorption mechanism of PEO to silica particles is the hydrogen bonding between the ether oxygen of PEO and isolated silanol groups on the silica surface (30-32). Likewise, hydroxyl groups on PVA can also provide hydrogen bonds for adsorption (33,34). In addition, carbon-based particles commonly used in desalination also exhibit weak adsorption due to van der Waals forces, even without strong hydrogen bonding. Despite the similar driving force for adsorption, the difference in molecular flexibility leads to a disparity in the adsorption state on particles.

Compared with the C–C single bond of PVA, the C–O single bond on PEO main chain corresponds to a lower potential barrier of internal rotation, resulting in a smaller rigid factor, making PEO more flexible than PVA. Owing to the better flexibility, it was easier for PEO to transform from random coils to an adsorbed conformation through internal rotation. The adsorbed conformation can be described as segments attached to the particle surface, loops of segments that extend into the solution between the chains, and tails of dangling ends of the chains (35). PVA with poor flexibility preferred extended loops and dangling tails to generate polymer bridging, through which two or more particles are linked together, thereby producing effective flocculation

$$(a) \longrightarrow (b) \longrightarrow (0)$$

**Figure 2:** Molecular structure of polymer binders: (a) rigid PVA and (b) flexible PEO.

and forming a crosslinked microstructure (36,37). When sheared, shear-thinning was observed due to the destruction of microstructure.

However, PEO tends to completely cover the particle surfaces due to the flexible chain. Repulsion between adsorbed layers made the suspensions to be thermodynamically stable and prevented flocculation (38–41). Therefore, the suspension remained Newtonian fluid since there is no microstructure destruction. Under the conditions where the particle surfaces are highly covered with adsorbed polymer, the colloidal interactions between particles are very weak. Reflected in the flow curve, the viscosity of PEO samples with the same filler addition has always been lower than that of PVA.

With the addition of silica less than 25%w/w, the shear rate dependence of viscosity for PVA/SiO<sub>2</sub> was nearly a Newtonian fluid. As the concentration of silica reached 25%w/w, the viscosity decreases as the shear rate increases, and the suspension begins to show a slight shear-thinning behavior. Moreover, the shear-thinning tendency is progressively pronounced with the increasing particle concentration. Shear-thinning can be attributed to the shear-induced breakdown of flocculated structures (42.43).

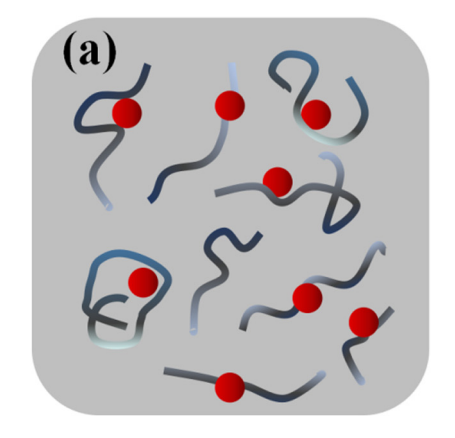
For typical flocculated suspensions, polymer bridges the particles together, forming a partial flocculated structure (Figure 3a), and a whole flocculation network forms when the number of bridges reaches a critical level (Figure 3b). It is generally believed that bridging flocculation occurs for long polymer chains and low surface coverage of particles (44,45). This requires enough uncovered particles in the range of bridging distance to form effective bridging flocculation. Above a critical concentration (~25%w/w), increasing the number of particles within the bridging distance, analogous to introducing more cross-linking agent, requires greater shear to destroy the network, resulting in large shear stress

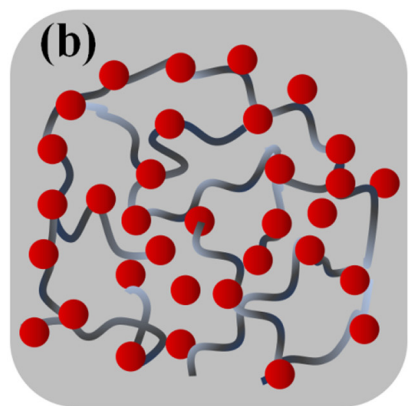
as shown in Figure 1(b). When the particle concentration is below a critical concentration, full coverage of polymer on the particle surface is achieved, and the suspensions can be sterically stabilized by polymer chains. Although flocculation occurs locally, the number of bare particles is not enough to form a cross-linked network via bridging. Therefore, the suspension is Newtonian fluid or slightly shear thinning caused by local microstructure destruction.

## 3.2 Dynamic rheological behavior of suspensions

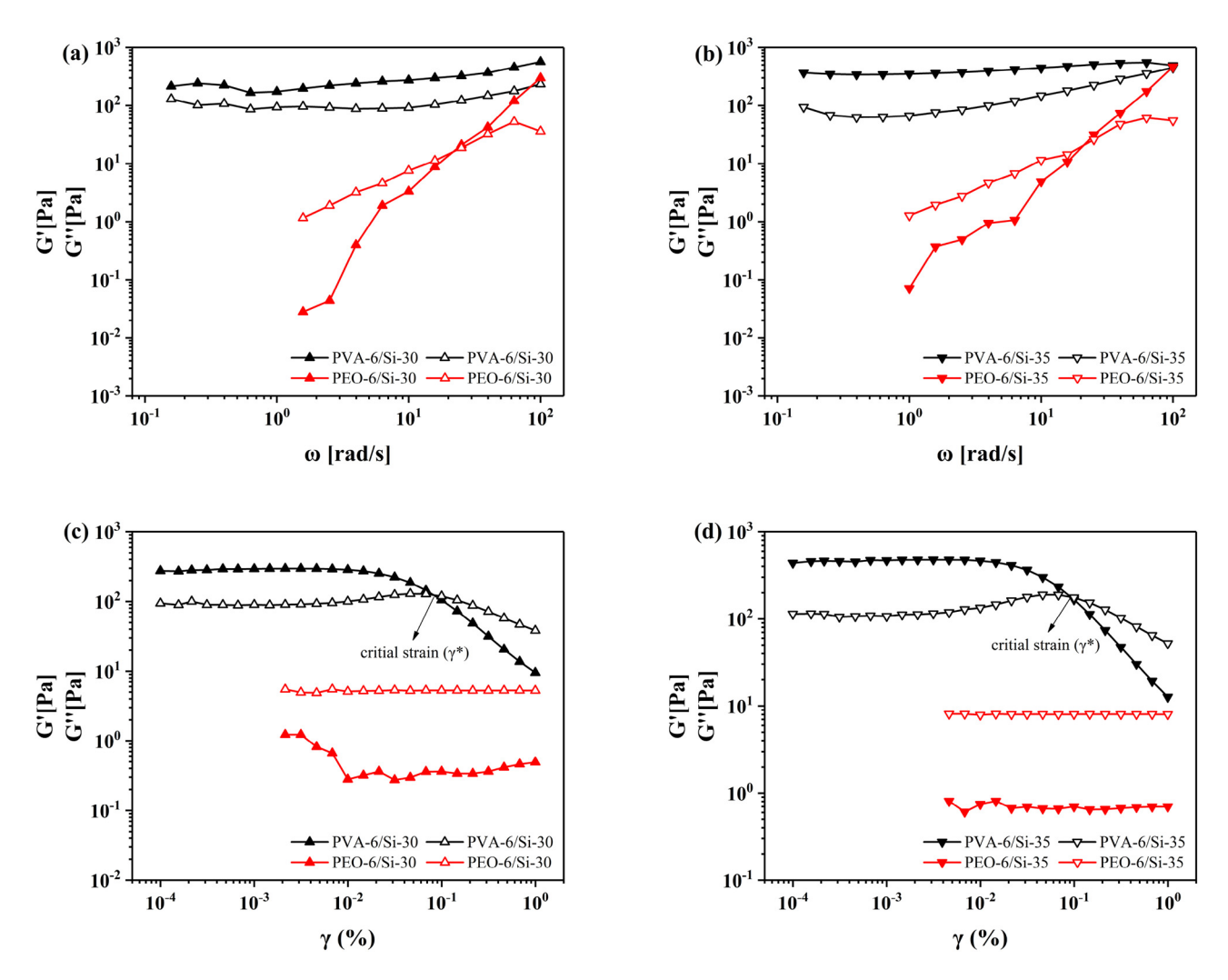
Dynamic test focuses on the mechanical properties of suspensions. To further detect the change in microstructure under shear, frequency sweep and amplitude sweep were used on PVA/SiO<sub>2</sub> and PEO/SiO<sub>2</sub> suspensions. Figure 4(a) and (b) shows the storage modulus (G') and loss modulus (G") measured by frequency sweep with an amplitude of 0.1%. It can be observed that for PVA/SiO<sub>2</sub>, G' is greater than G" in the whole range and shows little dependence on frequency, indicating a solid-like structure and the formation of a cross-linked network in the suspension. On the contrary, for PEO/SiO<sub>2</sub>, G" is greater than G' at low frequency and increases as the frequency increases, indicating a viscous fluid and a wrapping structure in the suspension. Meanwhile, these reasons also lead to the instability of G data in the low-frequency region (these data have been omitted for clarity).

Figure 4(c) and (d) shows the G' and G'' measured by amplitude sweep with an angular frequency of 6.28 s<sup>-1</sup>. For PVA/SiO<sub>2</sub>, there existed a critical value in strain, critical strain ( $\gamma^*$ ), at which G' was equal to G'', intersection of the two curves. Below  $\gamma^*$ , G' was greater than G'' and barely changed as the strain increased, indicating the presence of





**Figure 3:** Schematic representation of the two roles played by particle concentration in a polymeric suspension: (a) steric stabilization at low particle concentration and (b) bridging flocculation at high particle concentration.



**Figure 4:** Storage modulus (G') represented by solid symbols and the loss modulus (G'') represented by open symbols, as a function of angular frequency and shear strain for PVA/SiO<sub>2</sub> and PEO/SiO<sub>2</sub> suspensions with varying particle concentrations: (a) moduli vs angular frequency for 30%w/w, (b) moduli vs angular frequency for 35%w/w, (c) moduli vs shear strain for 30%w/w, and (d) moduli vs shear strain for 35%w/w.

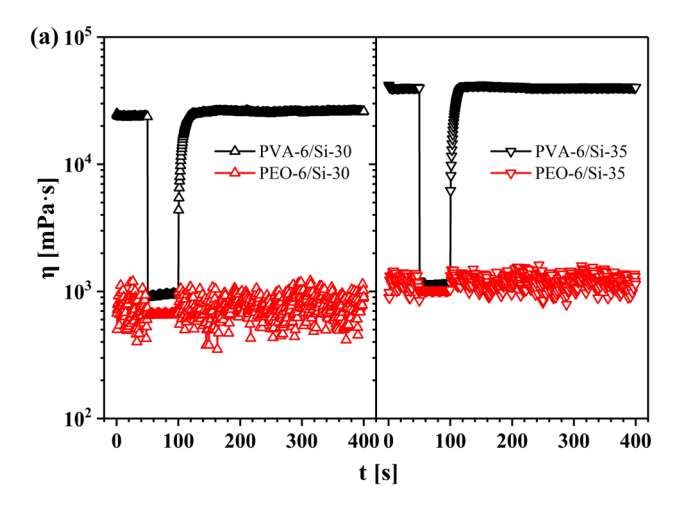
cross-linked network in PVA/SiO<sub>2</sub>. However, as strain increased near  $\gamma^*$ , G decreased rapidly, down to lower than G'. The critical strain point reflects the transformation from solid-like to liquid. This transformation indicates the breakdown of the cross-linked flocculated structures as it cannot withstand tensile stress. However, a similar transformation was not observed in PEO/SiO<sub>2</sub>, and G was lower than G'' in the whole range, indicating the absence of cross-linked structures in the suspension. These findings are consistent with the flow curve results presented earlier.

## 3.3 Thixotropic behavior of suspensions

Thixotropy, which is helpful for maintaining the shape and thickness after coating, is regarded as the evidence of cross-linking. As shown in Figure 5(a), 3ITT under the Rot-Rot-Rot mode was performed to investigate the viscosity recovery on time, wherein continuous shear measurements at alternating small and large shear rate were carried out. From the flow curve above, PVA/SiO<sub>2</sub> was shear-thinning fluid, so it can be seen that the viscosity decreased noticeably from the first low shear stage to the high shear stage. Then as the shear rate decreased to 0.5 s<sup>-1</sup>, the viscosity began to recover, returning to its initial value in approximately 30 s. Since viscosity rooted in the cross-linked structure, fast recovery of viscosity meant fast rebuilding of cross-linking. On the other hand, for PEO/SiO<sub>2</sub>, the viscosity remained approximately the same in all three stages, indicating the absence of cross-linking in the suspension.

From the hysteresis loop measurement in Figure 5(b), for PVA/SiO<sub>2</sub>, yielding was obvious in the shear-up curve, stress did not increase linearly, and the rate of increasing

6 — Hao Ming et al. DE GRUYTER



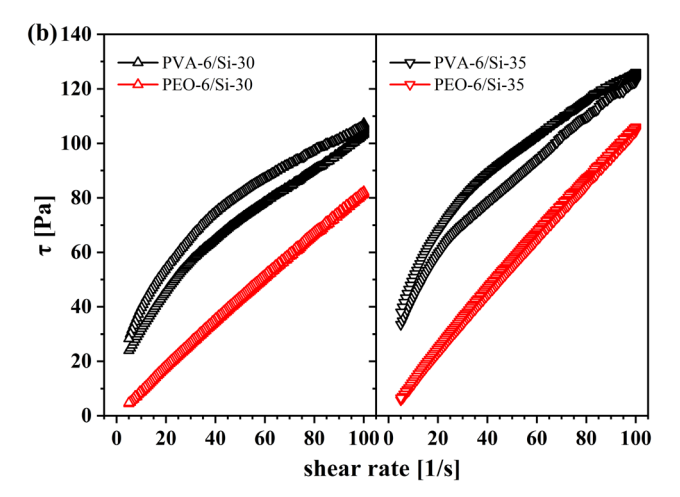


**Figure 5:** Thixotropic behavior of PVA/SiO $_2$  and PEO/SiO $_2$  suspensions: (a) 3ITT and (b) hysteresis loops.

decreased (the rate is equivalent to viscosity). In contrast, in the shear-down curve, stress decreased linearly in the high shear rate range. Then the viscosity increased as the shear rate decreased due to the rebuilding of the crosslinking. The recovery of viscosity came in sight during the shear going down rather than shear completely removed, illustrating that the destruction and rebuilding of the network were dynamically competing, which existed all through the shear process. This may be the reason for the fast recovery of viscosity. While, for PEO/SiO2, the shear-down curve almost superimposed on the shear-up curve, showing a linear increase or decrease. This typical rheological behavior of Newtonian fluid draws a conclusion that the microstructure barely changed under shear. Flexible polymers such as PEO are adsorbed and coated on particles at multiple points, making it challenging to pull away from all sites at the same time, especially in cases of multi-point adsorption with high coverage (46). Therefore, the enveloped structure was difficult to be destroyed under short time and low shear, resulting in no shear-thinning observed.

# 3.4 Influence of rheological behavior on coating

When particle-filled polymeric suspensions are used in a coating process, the viscosity needs to be within a suitable range. We define this range as "processing viscosity window." High viscosity (~10<sup>4</sup> mPa·s) was too thick to flow smoothly, leaving "brushmark" on the electrode surface (Figure 6a,

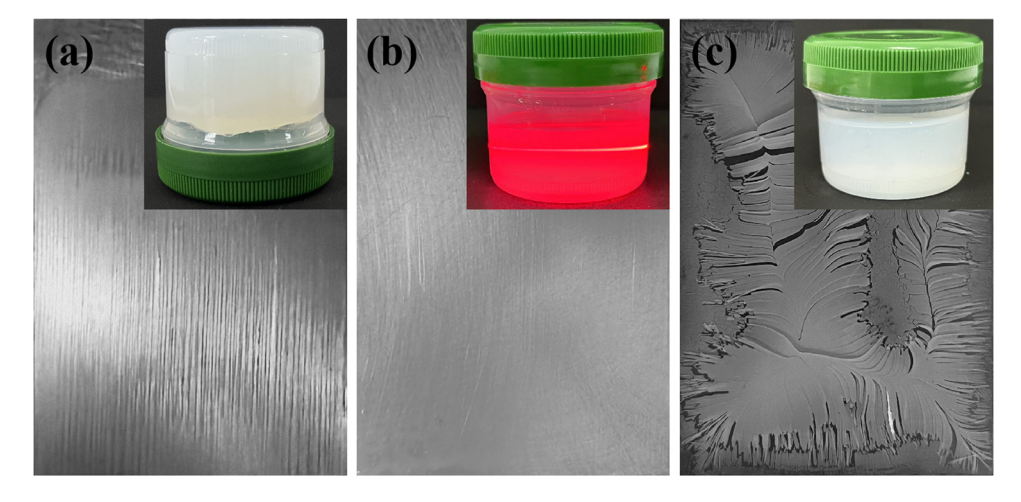


**Figure 6:** Digital photos of coatings prepared from suspensions with different rheologies: (a) high viscosity leaving "brushmark" from PVA-6/Si-35 suspension, (b) suitable viscosities such as PVA-6/Si-25 with Tyndall effect in suspension, and (c) encapsulated structure of PEO-6/Si-30 is prone to cracking.

PVA-6/Si-35), which will deteriorate not only the appearance but also the uniformity and performance in desalination. Low viscosity suspension (~10<sup>2</sup> mPa·s) spread easily, but causes problems in controllability of size and thickness, and the effective particles are prone to precipitation, which also increases the drying time of the electrode. To obtain a smooth and uniform electrode, low viscosity in coating and high viscosity in drying was profitable. Thus, appropriate shear-thinning is beneficial for molding through the coating method.

Appropriate shear thinning results from the formation and destruction of the internal network structure in the suspension. In the PVA/SiO<sub>2</sub> suspension, particles are linked together by polymers forming a strong network structure. Thixotropic test results also indicate that fast recovery of viscosity and fast rebuilding of cross-linked structure during subsequent drying process guaranteed the formation of network before most of the solvent evaporated. This was beneficial for coating method. The remaining high-strength network was enough to override the capillary force during evaporation, obtaining a robust coating on the current collector (Figure 6b, PVA-6/Si-25).

However, the viscosity of PEO/SiO2 is slightly lower than that of PVA at the same amount of particle addition. For example, the viscosity of PEO-6/Si-30 is close to that of PVA-6/Si-25. Although most PEO samples are also within the "processing viscosity window," the flexible chain of PEO is adsorbed and covered on filler particle surfaces. The suspension can be sterically stabilized and uniformly distributed by steric effects of polymer chains. In this case, although partial flocculation may occur, the wrapping structure is not enough to form an overall cross-linked network through bridging flocculation, resulting in a weak mechanical strength of the coating. At the same time, the strength of the stacked structure formed by encapsulated particles was not sufficient to withstand the capillary force, leading to cracking of the coating after drying (Figure 6c, PEO-6/Si-30). Obviously, a coating with crack morphology cannot be applied for CDI.

#### 4 Conclusions

Two silica suspensions with PVA and PEO were used to investigate the influence of polymer structure to coating through rheological method. PVA/SiO<sub>2</sub> exhibited shear-thinning, whose viscosity decreased as shear rate increased. While PEO/SiO<sub>2</sub> was a typical Newtonian fluid, whose viscosity barely changed. This is attributed to the difference

between the cross-linked structure of PVA/SiO2 and the encapsulation structure of PEO/SiO<sub>2</sub>. Rigid polymer, PVA, preferred conformation easy to generate bridging, which linked particles together producing flocculation and forming cross-linked microstructure. However, flexible polymer, PEO, tended to envelop the particles, preventing flocculation by repulsion between adsorbed layers. When sheared, crosslinked microstructure destruction in PVA/SiO2 resulted in shear-thinning, but PEO/SiO2 remained Newtonian fluid due to the absence of crosslinking. Thixotropic results of PVA/SiO<sub>2</sub> showed fast recovery of viscosity rooted in the fast rebuilding of cross-linked microstructure, while no shear-thinning and recovery were observed in PEO/SiO<sub>2</sub>.

Based on the rheological behavior of the two suspensions selected, the one with cross-linked microstructure was suitable because of the shear-thinning property. During the coating process, shear-thinning gave a low viscosity, avoiding "brushmark" on the surface of the coating. Then in the subsequent drying process, fast recovery of viscosity prevented spreading and contributed to the controllability of thickness. Meanwhile, fast rebuilding of the cross-linked structure achieved the formation of the network before the solvent completely evaporated. Additionally, we summarized the requirements for flocculation to form cross-linking: interaction between polymer and filler particles, sufficient amount of bare particles, and rigid polymer chains appropriate to adsorb on particle surface but not completely envelop the particles.

Funding information: It is a pleasure to acknowledge the generous financial support of this research by Scientific research fund project of Liaoning Provincial Department of Education (LJKMZ20220499, LQGD2020014, LJKQZ20222299), "Jie Bang Gua Shuai" Key Technologies R&D Program of Liaoning Province (2021JH1/10400031), LiaoNing Revitalization Talents Program (XLYC2007170).

**Author contributions:** Hao Ming: writing – original draft, formal analysis; Yinyan Guan: methodology, formal analysis; Cong Geng: investigation; Yingjun Gao: visualization; Jing Meng: project administration; Jiyan Liang: writingreview & editing, resources.

**Conflict of interest:** Authors state no conflict of interest.

Data availability statement: The experimental data and analysis results exhibited in this study are original and have been contributed by all authors. The corresponding author can make this information available to interested parties upon providing a reasonable justification.

### References

- Sun KG, Tebyetekerwa M, Wang C, Wang XF, Zhang XW, Zhao XS. Electrocapacitive deionization: mechanisms, electrodes, and cell designs. Adv Funct Mater. 2023;33(18):2213578. doi: 10.1002/adfm. 202213578.
- (2) Liu MJ, He MY, Han JL, Sun YY, Jiang H, Li Z, et al. Recent advances in capacitive deionization: research progress and application prospects. Sustainability. 2022;14(21):14429. doi: 10.3390/su142114429.
- (3) Bao SX, Xin CF, Zhang YM, Chen B, Ding W, Luo YP. Application of capacitive deionization in water treatment and energy recovery: a review. Energies. 2023;16(3):1136. doi: 10.3390/en16031136.
- (4) Geng C, Lv JY, Ming H, Liu SY, Gao YJ, Meng J, et al. Preparation of activated carbon electrode for capacitive deionization based on PTFE emulsion spraying technology. J Mater Sci. 2023;58(8):3825–36. doi: 10.1007/s10853-022-07941-y.
- (5) Kumar S, Aldaqqa NM, Alhseinat E, Shetty D. Electrode materials for desalination of water via capacitive deionization. Angew Chemie-Int Ed. 2023;62(35):e2023021. doi: 10.1002/anie.202302180.
- (6) Qiu Y, Zhang CJ, Zhang R, Liu ZY, Yang HZ, Qi S, et al. Integration of pore structure modulation and B, N co-doping for enhanced capacitance deionization of biomass-derived carbon. Green Energy Environ. 2023;8(5):1488–500. doi: 10.1016/j.gee.2023.01.005.
- (7) Song X, Fang DZ, Huo SL, Li KX. 3D-ordered honeycomb-like nitrogen-doped micro-mesoporous carbon for brackish water desalination using capacitive deionization. Environ Sci-Nano. 2021;8(8):2191–203. doi: 10.1039/d1en00276g.
- (8) Duan F, Du X, Li YP, Cao HB, Zhang Y. Desalination stability of capacitive deionization using ordered mesoporous carbon: effect of oxygen-containing surface groups and pore properties. Desalination. 2015;376:17–24. doi: 10.1016/j.desal.2015.08.009.
- (9) Park BH, Choi JH. Improvement in the capacitance of a carbon electrode prepared using water-soluble polymer binder for a capacitive deionization application. Electrochim Acta. 2010;55(8):2888–93. doi: 10.1016/j.electacta.2009.12.084.
- (10) Kim HS, Sohn JY, Hwang IT, Shin J, Jung CH, Son WK, et al. Electron beam-based fabrication of crosslinked hydrophilic carbon electrodes and their application for capacitive deionization. RSC Adv. 2019;9(17):9684–91. doi: 10.1039/c8ra10527h.
- (11) Liu K, Chen BB, Feng AH, Wu J, Hu XB, Zhou JE, et al. Bio-composite nanoarchitectonics for graphene tofu as useful source material for capacitive deionization. Desalination. 2022;526:115461. doi: 10. 1016/j.desal.2021.115461.
- (12) Feng JH, Xiong S, Wang Y. Atomic layer deposition of TiO<sub>2</sub> on carbon-nanotube membranes for enhanced capacitive deionization. Sep Purif Technol. 2019;213:70–7. doi: 10.1016/j.seppur.2018. 12.026.
- (13) Yang CM, Choi WH, Na BK, Cho BW, Cho WI. Capacitive deionization of NaCl solution with carbon aerogel-silica gel composite electrodes. Desalination. 2005;174(2):125–33. doi: 10.1016/j.desal.2004. 09.006.
- (14) Hackl L, Tsai SW, Kalyan B, Hou CH, Gadgil A. Electrically regenerated ion-exchange technology: leveraging faradaic reactions and assessing the effect of co-ion sorption. J Colloid Interface Sci. 2022;623:985–91. doi: 10.1016/j.jcis.2022.05.104.
- (15) Geng C, Gao YJ, Ming H, Duan DS, Meng J, Gao WC, et al. Continuous cycling of carbon-based capacitive deionization systems: an evaluation of the electrode performance and stability. J Electroanalytical Chem. 2022;914:116298. doi: 10.1016/j.jelechem. 2022.116298.

- (16) Hussain H, Jilani A, Salah N, Alshahrie A, Memić A, Ansari MO, et al. Freestanding activated carbon nanocomposite electrodes for capacitive deionization of water. Polymers. 2022;14(14):2891. doi: 10.3390/polym14142891.
- (17) Weng JZ, Wang SY, Wang G, Zhang PX, Lu B, Wang HL, et al. Carbon electrode with cross-linked and charged chitosan binder for enhanced capacitive deionization performance. Desalination. 2021;505;114979. doi: 10.1016/i.desal.2021.114979.
- (18) Venkatesan G, Pauline S. Influence of chemical, electrochemical exfoliation, hydrophilic, and hydrophobic binder on the sorption capacity of graphene in capacitive deionization. J Environ Eng. 2022;148(7):04022033. doi: 10.1061/(ASCE)EE.1943-7870.0001999.
- (19) Park BH, Kim YJ, Park JS, Choi J. Capacitive deionization using a carbon electrode prepared with water-soluble poly(vinyl alcohol) binder. J Ind Eng Chem. 2011;17(4):717–22. doi: 10.1016/j.jiec.2011. 05.015.
- (20) Thom NT, Anh VTK, Trang NTT, Phuong NT, Thanh DTM, Dang LH, et al. Study on the functionalization of activated carbon and the effect of binder toward capacitive deionization application. Green Process Synth. 2022;11(1):830–41. doi: 10.1515/qps-2022-0049.
- (21) Jain A, Kim J, Owoseni OM, Weathers C, Caña D, Zuo KC, et al. Aqueous-processed, high-capacity electrodes for membrane capacitive deionization. Environ Sci Technol. 2018;52(10):5859–67. doi: 10.1021/acs.est.7b05874.
- (22) Huang D, Hu Z, Liu T, Lu B, Zhen Z, Wang G, et al. Seawater degradation of PLA accelerated by water-soluble PVA. e-Polymers. 2020;20(1):759–72. doi: 10.1515/epoly-2020-0071.
- (23) Heck CA, von Horstig MW, Huttner F, Mayer JK, Haselrieder W, Kwade A. Review-knowledge-based process design for high quality production of NCM811cathodes. J Electrochem Soc. 2020;167(16):160521. doi: 10.1149/1945-7111/abcd11.
- (24) Srimuk P, Su X, Yoon J, Aurbach D, Presser V. Charge-transfer materials for electrochemical water desalination, ion separation and the recovery of elements. Nat Rev Mater. 2020;5(7):517–38. doi: 10.1038/s41578-020-0193-1.
- (25) Tang KX, Yiacoumi S, Li YP, Tsouris C. Enhanced water desalination by increasing the electroconductivity of carbon powders for high performance flow-electrode capacitive deionization. ACS Sustain Chem Eng. 2018;7:1085–94. doi: 10.1021/acssuschemeng.8b04746.
- (26) Akuzum B, Singh P, Eichfeld DA, Agartan L, Uzun S, Gogotsi Y, et al. Percolation characteristics of conductive additives for capacitive flowable (semi-solid) electrodes. ACS Appl Mater Interfaces. 2020;12:5866–75. doi: 10.1021/acsami.9b19739.
- (27) You W, Yu W. Slow linear viscoelastic relaxation of polymer nanocomposites: contribution from confined diffusion of nanoparticles. Macromolecules. 2019;52(23):9094–104. doi: 10.1021/acs. macromol.9b01538.
- (28) Tsagaropoulos G, Eisenberg A. Dynamic mechanical study of the factors affecting the two glass transition behavior of filled polymers. Similarities and differences with random ionomers. Macromolecules. 1995;28(18):6067–77. doi: 10.1021/ma00122a011.
- (29) Saito Y, Hirose Y, Otsubo Y. Effect of poly(ethylene oxide) on the rheological behavior of silica suspensions. Rheol Acta. 2011;50:291–301. doi: 10.1007/s00397-010-0523-0.
- (30) Rubio J, Kitchener JA. The mechanism of adsorption of poly(ethylene oxide) flocculant on silica. J Colloid Interface Sci. 1976;57:132–42. doi: 10.1016/0021-9797(76)90182-x.
- (31) Zhou SZ, Qiao XG. Synthesis of raspberry-like polymer@silica hybrid colloidal particles through biphasic sol-gel process. Colloids Surf A. 2018;553:230–6. doi: 10.1016/j.colsurfa.2018.05.040.

- (32) Wang DP, Yang MQ, Dong ZX, Bo SQ, Ji XL. Interaction between poly (ethylene oxide) and silica nanoparticles in dilute solutions. Chin J Polym Sci. 2013;31(9):1290–8. doi: 10.1007/s10118-013-1321-9.
- (33) Panigrahi R, Chakraborty S, Ye J, Lim GS, Lim FCH, Yam JKH, et al. Elucidating the role of interfacial hydrogen bonds on glass transition temperature change in a poly(vinyl alcohol)/SiO₂ polymernanocomposite by noncovalent interaction characterization and atomistic molecular dynamics simulations. 2020;40(21):2000240. doi: 10.1002/marc.202000240.
- (34) Kumari A, Singh RK, Kumar N, Kumari R, Sharma S. Green synthesis and physical properties of crystalline silica engineering nanomaterial from rice husk (agriculture waste) at different annealing temperatures for its varied applications. J Indian Chem Soc. 2023;100(5):100982. doi: 10.1016/j.jics.2023.100982.
- (35) Otsubo Y. Rheological behavior of suspensions flocculated by weak bridging of polymer coils. J Colloid Interface Sci. 1999;215:99–105. doi: 10.1006/jcis.1999.6252.
- (36) Kim S, Hyun K, Moon JY, Clasen C, Ahn KH. Depletion stabilization in nanoparticle-polymer suspensions: multi-length-scale analysis of microstructure. Langmuir. 2015;31(6):1892–900. doi: 10.1021/ la504578x.
- (37) Kim S, Sung JH, Ahn KH, Lee SJ. Drying of the silica/PVA suspension: effect of suspension microstructure. Langmuir. 2009;25(11):6155–61. doi: 10.1021/la804112b.
- (38) Zhang Q, Archer LA. Poly(ethylene oxide)/silica nanocomposites: structure and rheology. Langmuir. 2002;18(26):10435–42. doi: 10.1021/la026338j.

- (39) Wang J, Heuer L, Joseph D. Aging properties of semidilute aqueous solutions of polyethylene oxide seeded with silica nanoparticles. J Rheol. 2005;49(6):1303–16. doi: 10.1122/1.2072007.
- (40) Zhao WW, Su YL, Gao X, Xu JJ, Wang DJ. Interfacial effect on confined crystallization of poly(ethylene oxide)/silica composites. J Polym Sci Part B: Polym Phys. 2016;54(3):414–23. doi: 10.1002/polb.23915.
- (41) Power AJ, Papananou H, Rissanou AN, Labardi M, Chrissopoulou K, Harmandaris V, et al. Dynamics of polymer chains in poly(ethylene oxide)/silica nanocomposites via a combined computational and experimental approach. J Phys Chem B. 2022;126(39):7745–60. doi: 10.1021/acs.jpcb.2c04325.
- (42) Otsubo Y. Effect of surfactant adsorption on the polymer bridging and rheological properties of suspensions. Langmuir. 1994;10(4):1018–22. doi: 10.1021/la00016a011.
- (43) Otsubo Y. Effect of adsorption affinity of polymers on the viscosity behavior of suspensions. J Colloid Interface Sci. 1998;204(1):214–6. doi: 10.1006/jcis.1998.5567.
- (44) Growney DJ, Mykhaylyk OO, Derouineau T, Fielding LA, Smith AJ, Aragrag N, et al. Star diblock copolymer concentration dictates the degree of dispersion of carbon black particles in nonpolar media: bridging flocculation versus steric stabilization. Macromolecules. 2015;48(11):3691–704. doi: 10.1021/acs.macromol.5b00517.
- (45) Saito Y, Ogura H, Otsubo Y. Rheological behavior of silica suspensions in aqueous solutions of associating polymer. Colloid Polym Sci. 2008;286(13):1537–44. doi: 10.1007/s00396-008-1928-5.
- (46) Otsubo Y. Rheology control of suspensions by soluble polymers. Langmuir. 1995;11(6):1893–8. doi: 10.1021/la00006a013.